
Article:
Wang, J.G., Li, Z.C., Zhang, Z.Y. et al. (2026) Decay properties of new isotopes 235Bk and 231Am. Physics Letters B. 140365. ISSN: 0370-2693

https://doi.org/10.1016/j.physletb.2026.140365

Phys. Lett. B 875 (2026) 140365

Contents lists available at ScienceDirect

Physics Letters B

journal homepage: www.elsevier.com/locate/physletb

Letter

Decay properties of new isotopes ^{235}Bk and ^{231}Am

J.G. Wang [a,b], Z.C. Li [a,b], Z.Y. Zhang [a,b,*], Z.G. Gan [a,b,c,*], A.N. Andreyev [d,e], M.H. Huang [a,b,c], L. Ma [a,b,c], M.M. Zhang [a,b], H.B. Yang [a,b], C.L. Yang [a,b], Y.H. Qiang [a,b], Z.H. Li [a,b], X.Y. Huang [a,b], G. Xie [a,b], L. Zhu [a,b], H. Zhou [a,b], X. Zhang [a,b], J.H. Zheng [a,b], S.Y. Xu [a,b], Z. Zhao [a,b], L.C. Sun [a,f], F. Guan [a,g], X.L. Wu [a,c], W.X. Huang [a,b,c], Y.L. Tian [a,b,c], Y.S. Wang [a,c], J.Y. Wang [a,c], Z.W. Lu [a], Y. He [a,b], L.T. Sun [a,b], Z.Z. Ren [h], S.G. Zhou [b,i], V.K. Utyonkov [j], A.A. Voinov [j], Yu.S. Tsyganov [j], A.N. Polyakov [j]

[a] State Key Laboratory of Heavy ion science and Technology, Institute of Modern Physics, Chinese Academy of Sciences, 730000, Lanzhou, China
[b] School of Nuclear Science and Technology, University of Chinese Academy of Sciences, 100049, Beijing, China
[c] Advanced Energy Science and Technology Guangdong Laboratory, 516000, Huizhou, China
[d] School of Physics, Engineering and Technology, University of York, YO10 5DD, York, United Kingdom
[e] Advanced Science Research Center Japan Atomic Energy Agency, 819-1195, Tokai, Ibaraki, Japan
[f] School of Space Science and Physics, Shandong University, 264209, Weihai, China
[g] Guangxi Key Laboratory of Nuclear Physics and Technology, Guangxi Normal University, 541004, Guilin, China
[h] School of Physics Science and Engineering, Tongji University, 200092, Shanghai, China
[i] Institute of Theoretical Physics, Chinese Academy of Sciences, 100190, Beijing, China
[j] Joint Institute for Nuclear Research, RU-141980, Dubna, Russian Federation

ARTICLE INFO

Editor: H Gao

PACS:
21.10.Dr
23.60.+e
25.60.Pj
29.17.+w
29.30.-h

Keywords:
New isotope
Neutron-deficient nuclei
α decay
Gas-filled recoil separator

ABSTRACT

The new isotopes, ^{235}Bk and its α-decay daughter ^{231}Am, were investigated using the gas-filled recoil separator SHANS2. They were identified by measuring radioactive decay chains originating from ^{235}Bk, which was produced via the ^{197}Au(^{40}Ar, 2n)^{235}Bk reaction. Three correlated α-decay chains were assigned to ^{235}Bk, from which the α-particle energy of ^{235}Bk was measured to be 7632(17) keV. For ^{231}Am, the α-particle energy and half-life were determined to be 7109(18) keV and 75^{+137}_{-30} s, respectively. The α-decay branching ratio of ^{231}Am was evaluated as 17^{+65}_{-15}%. A systematic analysis reveals significant discrepancies between the experimental data and the WS4 + RBF theoretical predictions for the isotopes of Bk and Am, which warrant further investigation.

1. Introduction

The synthesis of new isotopes provides valuable information on nuclear mass and structural properties. For nuclei with proton numbers $Z > 92$, the shell correction plays an essential role in stabilizing nuclei by raising fission barriers (B_f). However, for these heavy nuclei far from closed shells, the shell correction weakens and B_f decreases rapidly, making such nuclei more difficult to be synthesized and studied experimentally.

For neutron-deficient berkelium and americium isotopes with $N \sim 138$, a region lying between the $N = 126$ and $N = 152$ shell closures, theoretical calculations predict the fission barrier height B_f is below 4 MeV [1,2]. Meanwhile, mass tables suggest that the Q-values of electron capture (EC) in this region typically exceed 4 MeV [3,4]. The large Q_{EC} and positive $Q_{EC} - B_f$ values imply the coexistence and competition of multiple decay modes in this region, including EC decay, α decay, spontaneous fission (SF), and electron capture delayed fission (ECDF) [5–7]. These rich structural and decay phenomena

* Corresponding authors.
E-mail addresses: zhangzy@impcas.ac.cn (Z.Y. Zhang), zggan@impcas.ac.cn (Z.G. Gan).

https://doi.org/10.1016/j.physletb.2026.140365
Received 29 September 2025; Received in revised form 20 January 2026; Accepted 15 March 2026
Available online 17 March 2026

provide critical tests for theoretical models in the neutron-deficient heavy nuclei.

In previous experimental studies, β^+/EC decay has been identified as the dominant decay mode for neutron-deficient americium isotopes $^{230,232-235}$Am [5,8–14], with the exception of ^{223,229}Am [15]. The ECDF mode has been observed only in the odd-odd isotopes ^{230,232,234}Am [5,12–14]. The ECDF probability (P_{ECDF}) increases sharply from 6.6×10^{-5} of ^{234}Am to > 0.3 of ^{230}Am which is the highest value reported so far among all known β-delayed fission nuclei [5,7–14]. Additionally, α decay has been observed in $^{233-235}$Am, albeit with low branching ratios (<6%) [8,9,13,14].

Experimental data on neutron-deficient berkelium isotopes are rare. The isotopes ^{236,238}Bk, produced through α decay of ^{240,242}Es [16,17], respectively, were found to decay predominantly via EC decay. The ECDF were also observed, with P_{ECDF} values of 0.04 for ^{236}Bk and 4.8×10^{-4} for ^{238}Bk. ^{234}Bk was synthesized directly using the fusion reaction ^{197}Au(^{40}Ar, 3n)^{234}Bk [10]. In that study, Kaji *et al.* reported the observation of α decay and β^+/EC decay in ^{234}Bk, although no branching ratios were provided.

In this work, we report the first identification of the new isotopes, ^{235}Bk and its α-decay daughter ^{231}Am, along with a study of their decay properties. Furthermore, a search for the potential ECDF and SF was conducted, but no fission event was found.

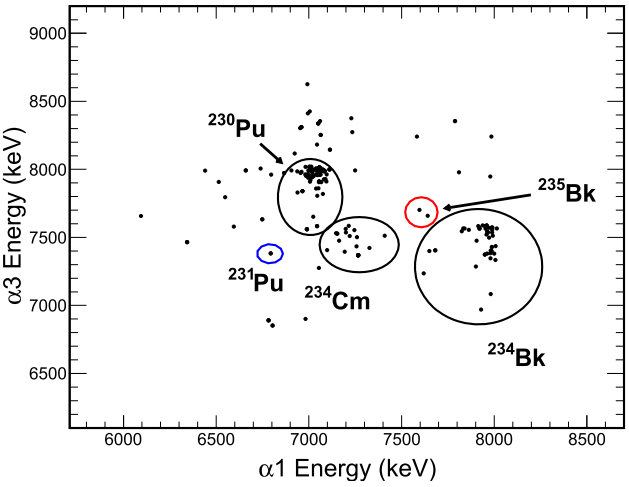

Fig. 1. Two-dimensional scatter plot of α-particle energies of parent and granddaughter nuclei for Imp-$\alpha1-\alpha2-\alpha3$ correlated events observed at beam energies of 182.4 and 187.5 MeV. The correlated events were searched using the following time windows: Δt(Imp-$\alpha1$) < 300 s, $\Delta t(\alpha1-\alpha2)$ < 500 s, and $\Delta t(\alpha2-\alpha3)$ < 2.5 s.

2. Experiment

The isotope ^{235}Bk was synthesized via the reaction ^{197}Au(^{40}Ar, 2n)^{235}Bk. The target ^{197}Au with an average thickness of 500 μg/cm^2 was deposited on a 60 μg/cm^2 carbon backing. Twenty arc-shaped targets were mounted on a rotating wheel with a diameter of 50 cm, rotating at 1800 rpm during the experiment. A beam of ^{40}Ar at energies of 182.4(10) and 187.5(10) MeV was provided by the China Accelerator Facility for superheavy Elements (CAFE2) [18] at the Institute of Modern Physics, Chinese Academy of Sciences, China. The beam energies at the middle of the target were 179.7 and 184.8 MeV, respectively. The total beam doses were 2.34×10^{18} and 3.29×10^{18} ions for the 182.4- and 187.5-MeV runs, respectively. Recoiling evaporation residues (ERs) were separated from the primary beam by the gas-filled recoil separator SHANS2 (Spectrometer for Heavy Atoms and Nuclear Structure-2) [18,19], which was filled with helium at a pressure of 100 Pa.

The ERs were subsequently implanted into a 300-μm-thick double-sided silicon strip detector (DSSD) located at the focal plane. The DSSD featured 48 horizontal strips on the front side (providing the y-position) and 128 vertical strips on the rear side (providing the x-position), each with a width of 1 mm. This arrangement formed a high-resolution pixel grid with 6144 pixels, enabling precise localization of each implantation and decay position through its (x, y) coordinates. The high granularity of the detector significantly reduced the probability of random correlation events. Due to the shallow implantation depth (a few μm) of ERs in the DSSD, fission fragments and α particles could escape the DSSD. To register these events, six single-sided silicon strip detectors (SSDs), each with a thickness of 500 μm and an active area of 120×63 mm^2 divided into eight 15-mm-wide strips, were arranged in an open-box geometry upstream of the DSSD. Events registered in both the DSSD and SSDs were classified as reconstructed events. By combining of the DSSD and SSD detectors, the detection efficiency increased from approximate 55% (geometric efficiency of DSSD) to 86(8)%. Three 300-μm-thick detectors with an active area of 50×50 mm^2 were mounted side-by-side behind the DSSD to veto high-energy light particles penetrating the DSSD. All silicon detectors were cooled by a liquid-alcohol system operating at −30°C. Two multi-wire proportional counters (MWPCs), placed approximate 20 cm upstream of the DSSD, were used to distinguish the ER implantation from the decay events. All signals were processed by preamplifiers and acquired by a 100-MHz-sampling 14-bit digitizer operating in self-triggered mode, recording energy, timestamp, and waveform data (20–30 μs in length). The data acquisition (DAQ) system timestamped each event using the Unix Epoch time. Further details of SHANS2 and the detector system are available in Ref. [19].

The silicon detectors were pre-calibrated using standard α sources (^{239}Pu, ^{241}Am, and ^{244}Cm). Then, they were re-calibrated by the α decay of ^{211}Ac, ^{207}Fr, ^{210}Ra, and ^{206}Rn isotopes that were produced in the ^{159}Tb(^{54}Cr, xn)$^{213-x}$Ac reaction conducted before this experiment. α-particle energies were adopted from the National Nuclear Data Center (NNDC) database [20]. The typical energy resolution (full width at half maximum, FWHM) was approximately 30 keV for 5–9 MeV α-particles detected in the DSSD, and ~80 keV for reconstructed events. Energy thresholds were set at ~100 keV for the DSSD and ~250 keV for the SSDs. Pileup signals were reprocessed during the offline analysis. For events with time intervals larger than 2.5 μs, energies were determined using a trapezoidal shaping algorithm [21], achieving an FWHM of approximately 35 keV. For signals separated with less than 2.5 μs, a dedicated fitting method [22] was applied to reconstruct the energy, resulting in FWHM values ranging from 45 to 70 keV depending on the time interval. For example, a resolution of ~48 keV was obtained for the short-lived decay of ^{217}Ra ($T_{1/2}$ = 1.6 μs).

Decay chains were identified by employing spatial and temporal correlation of implantation (Imp) and their subsequent decay events. The implantations and decay events were required to occur within a same pixel. For the events triggering two adjacent strips, decay correlations would be searched for in all possible neighboring pixels. For decay events, the energy difference between the front and rear side of DSSD ($E_x - E_y$) should be less than 300 keV. Under this condition, the average count rates were 0.12 Hz/pixel for 2–11 MeV implantation events. The high implantation rate limits the possibility to determine half-life of the nuclei with values longer than a few seconds. Therefore, the ER signal in the following is only referred to as the implantation event closest to the decay signal in a given pixel. The average count rates of decay events in the energy range of 0.1–3 and 6–12 MeV were 1.9×10^{-3} and 1.1×10^{-4} Hz/pixel, respectively, and that for reconstructed decay events in the range of 6–12 MeV was 4.5×10^{-6} Hz/pixel.

3. Results and discussion

Due to the lack of information on the daughter nucleus, a two-dimensional correlation plot of the parent (α_1) and granddaughter (α_3) nuclei is presented in Fig. 1. The following time windows were applied to search correlated events: Δt(Imp-$\alpha1$) < 300 s, $\Delta t(\alpha1-\alpha2)$ < 500 s, and $\Delta t(\alpha2-\alpha3)$ < 2.5 s. Here α n denotes the nth α particle detected in tem-

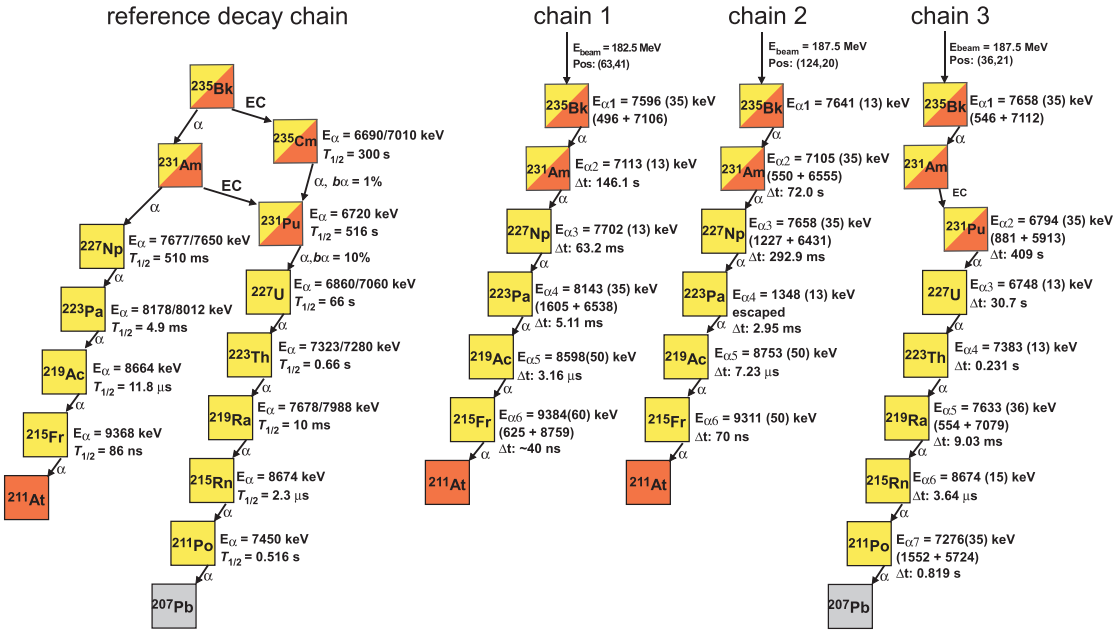

Fig. 2. Reference decay chain and observed α-decay chains of ^{235}Bk. The reference decay chain shows the potential decay pathways of ^{235}Bk, where the half-lives $T_{1/2}$, α-particle energies E_α, and α-decay branching ratios b_α of known nuclei are adopted from NNDC [20] and some recent literatures [23,24]. For the observed decay chains, the beam energies, implantation positions, measured α-particle energies E_α, and time intervals Δt between correlated signals are listed for each event. In the case of reconstructed events, the energies registered in both detectors are presented in parentheses, with the DSSD energy listed first. Due to the high implantation rate, the measured Δt(Imp-α1) values (20.96, 6.90, and 6.15 s for chains 1–3, respectively) cannot be reliably attributed to the decay time of ^{235}Bk, therefore they are not shown in the figure.

poral sequence following an implantation. By comparing with known α-decay properties, three dominant groups of correlated events, labeled by black ellipses, were assigned to ^{234}Bk [10]: (1) α decay: ^{234}Bk(α) $\rightarrow$ ^{230}Am(β^+/EC) $\rightarrow$ ^{230}Pu(α) $\rightarrow$ ^{226}U(α) decay chain, (2) β^+/EC decay: ^{234}Bk (β^+/EC) $\rightarrow$ ^{234}Cm(α) $\rightarrow$ ^{230}Pu(α) $\rightarrow$ ^{226}U(α) decay chain, (3) its subsequent nucleus ^{230}Pu: ^{230}Pu(α) $\rightarrow$ ^{226}U(α) $\rightarrow$ ^{222}Th(α) decay chain. Since the direct production cross-section of ^{230}Pu is negligible according to HIVAP calculations [25], the observed ^{230}Pu events can be attributed to either the missing α1 signal or random correlations with implantation signals, due to the high implantation rate and the long half-life.

Two new α-decay correlations, marked by a red circle in Fig. 1, were assigned to the new isotope ^{235}Bk. Details of these two decay chains (chains 1 and 2) are presented in Fig. 2. These α1 and α2 events exhibited very similar energies and the $\Delta t(\alpha 1 - \alpha 2)$ occurred within comparable time intervals. They were attributed to the α decays of ^{235}Bk and its α-decay daughter nucleus ^{231}Am, respectively. The α3 particles, with energies of 7702(13) and 7658(35) keV and time intervals $\Delta t(\alpha 2 - \alpha 3)$ of 63.2 and 292.9 ms, respectively, should be assigned to ^{227}Np based on previously reported values of E_α = 7650(21) and 7677(20) keV and $T_{1/2}$ = 510(60) ms [20,24,26]. According to previous studies [20,23,27,28], the expected subsequent α-decay chain should be ^{223}Pa (E_α = 8178/8012 keV, $T_{1/2}$ = 4.9 ms) $\rightarrow$ ^{219}Ac (E_α = 8664 keV, $T_{1/2}$ = 11.8 μs) $\rightarrow$ ^{215}Fr (E_α = 9368 keV, $T_{1/2}$ = 86 ns) as shown in reference decay chain in Fig. 2. Due to the very short decay time of ^{219}Ac and ^{215}Fr, the subsequent α4-α6 events of chains 1 and 2 should manifest as pulse pileup, as illustrated in Fig. 3(a) and (b). The energies and time intervals of these particles were extracted via a fitting method and the results were listed in corresponding chains in Fig. 2. In chain 2, the α4 was an escaped event for which only a portion of α energy was registered due to the limited detection efficiency of the silicon detectors. Given the background count rate for 0.1–3 MeV α-like decay events, it is unlikely that the α4 signal arose from random correlation within such a short time window. Although the energy uncertainties from the fitting method are relatively large due to the extremely short time intervals, the extracted values for the E_α and Δt are consistent with previous data in Refs. [20,23,27,28]. The distinct decay pattern starting from ^{227}Np provides unambiguous evidence that these two decay chains originate from ^{235}Bk.

Additionally, one α-decay correlation marked with a blue circle in Fig. 1 was attributed to ^{231}Pu, which originates from ^{235}Bk via the decay pathway of ^{235}Bk (α) $\rightarrow$ ^{231}Am (β^+/EC) $\rightarrow$ ^{231}Pu (α), as explained below. The measured α-decay chain following ^{231}Pu is displayed as α2 to α7 events in chain 3 of Fig. 2. The experimental energies and time intervals were in good agreement with the α-decay properties reported in Refs. [20,29], except for α7 decay from ^{211}Po. The α7 is a reconstructed event and its measured energy of 7276(35) keV was lower than previously reported value of 7450(5) keV. This discrepancy may be due to that the energy of escaped particle was registered by two adjacent strips in the SSD, where the energy in one strip fell below the detection threshold (~250 keV). Despite the lower energy, the α7 event, which was occured following a pileup event with Δt = 3.64 μs and E_α = 7633 and 8674 keV as shown in Fig. 3(c), should belong to ^{211}Po. Consequently, the α2 particle in chain 3 should be assigned to ^{231}Pu.

According to the HIVAP calculations [25], the direct production cross section of ^{231}Pu is strong suppressed. Therefore, ^{231}Pu should originate from the decay of ^{235}Bk via a pathway such as ^{235}Bk (α) $\rightarrow$ ^{231}Am (β^+/EC) $\rightarrow$ ^{231}Pu (α) or ^{235}Bk (β^+/EC) $\rightarrow$ ^{235}Cm (α) $\rightarrow$ ^{231}Pu (α) as indicated in the reference decay chain in Fig. 2. A search was conducted for candidate precursor decay signals within 2500 s before the α2 event. Twelve candidate events were identified, eleven of which had energies below 3 MeV. The event closest to α_2, with E = 362 keV and Δt = 244 s, is likely a random correlation due to the high count rate of low-energy decay signals. The second closest candidate was a reconstructed event with E_α = 7658(35) keV and Δt = 409 s. This energy is consistent with the $E_{\alpha 1}$ values of chains 1 and 2, and is at least 600 keV higher than the known α-particle energies of ^{235}Cm (6690(20) and 7010(20) keV) [30]. Meanwhile, the $\Delta t(\alpha 1 - \alpha 2)$ of 409 s is reasonable, considering the time intervals of α particles from ^{235}Bk and ^{231}Am of chains 1 and 2, along with the half-life of ^{231}Pu ($T_{1/2}$ = 516(30) s) [29]. The random probability for reconstructed events (E_α = 6–12 MeV) within 500 s was

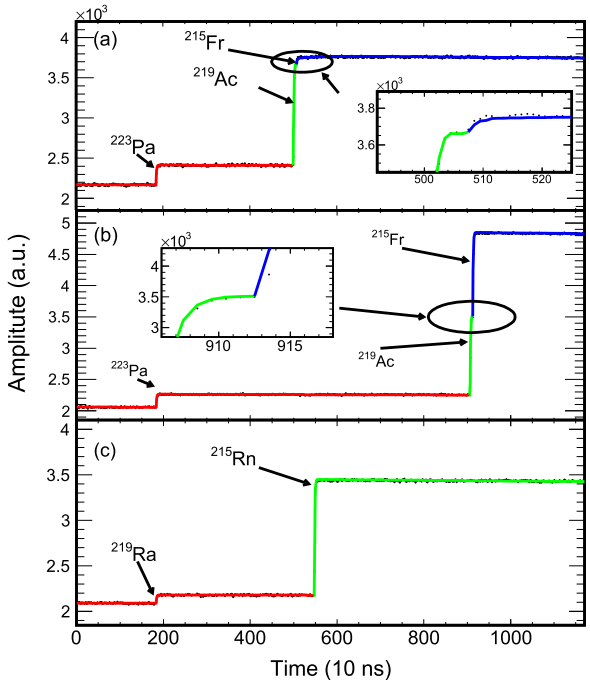

Fig. 3. Waveform traces of pileup events in the subsequent α-decay chains of ^{235}Bk. Traces (a) and (b) correspond to the α-decay sequences ^{223}Pa → ^{219}Ac → ^{215}Fr from chains 1 and 2 in Fig. 2, respectively. The insets magnify the pileup trace of ^{219}Ac and ^{215}Fr, which has a very short time interval. Trace (c) shows the α decay of ^{219}Ra → ^{215}Rn from chain 3 in Fig. 2. Black dots represent preamplifier signals traces, and colored lines are the corresponding fitting curves.

Table 1
Decay properties of ^{235}Bk and ^{231}Am. The Q_{EC} was deduced with use of the mass table [3] and Q_α in this work.

Nuclide	E_α (keV)	$T_{1/2}$(s)	Q_α (keV)	Q_{EC} (keV)
^{235}Bk	7632(17)	–	7764(17)	4417(128)
^{231}Am	7109(18)	75^{+137}_{-30}	7234(18)	3929(82)

calculated to be 2.45×10^{-3}. Therefore, this α particle was identified as the precursor event of ^{231}Pu and it should be attributed to ^{235}Bk rather than ^{235}Cm.

From the decay chains 1 and 2, the α-particle energy and half-life of ^{231}Am were determined as 7109(18) keV and 75^{+137}_{-30} s, respectively, using the low-statistics analysis method described in Ref. [31]. Assuming the α decay of ^{231}Am is the ground state (g.s.) to ground state transition, the corresponding Q_α and $Q_{\rm EC}$ were deduced to be 7234(18) and 3929(82) keV, respectively. As shown in chain 3, ^{231}Am can undergo EC decay to ^{231}Pu. Given the 10^{+7}_{-3}% α-decay branch of ^{231}Pu [29], the α-decay branching ratio of ^{231}Am was determined as 17^{+65}_{-15}%. Consequently, the partial α-decay half-life $T^{\alpha}_{1/2} = 441^{+803}_{-174}$ s was deduced.

The ground states of neutron-deficient $^{235-243}$Am isotopes have been assigned as $\pi5/2^-[523]$ orbits based on the experimental logft values, see [32] and references therein. Meanwhile, according to the FRDM2012 calculations [33], the g.s. spin and parity of ^{231}Am are predicted to be $5/2^-$. Based on the systematics and theoretical results, we tentatively assign the g.s. spin and parity of ^{231}Am as $(5/2^-)$. In addition, the g.s. spin of ^{227}Np is predicted to be 1/2 in Ref. [33]. As a result, the theoretical partial α-decay half-life $T^{\alpha}_{1/2} = 404$ s was calculated using the New Geiger-Nuttall law [34] with the assumption of $\Delta L = 2$. This value agrees well with the experimental result of 441^{+803}_{-174} s. Therefore, the reduced α-decay width $\delta^2 = 107^{+198}_{-43}$ keV of ^{231}Am was extracted as

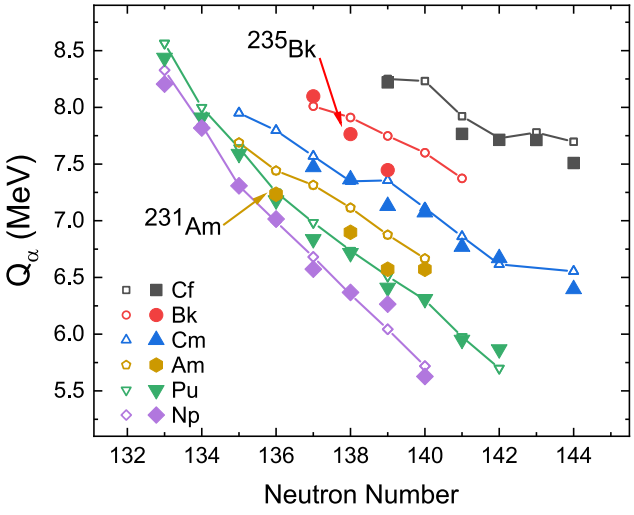

Fig. 4. Systematic comparison of maximum experimental Q_α with theoretical g.s-g.s. $Q^{\rm th}_\alpha$ for the neutron-deficient Np-Cf isotopes. The open symbols are the theoretical values obtained by the Weizsäcker-Skyrme (WS4) model together with the Radial Basis Function (RBF) corrections [36]. The solid symbols denote the experimental values, which were derived from measured maximum α-particle energies [20].

by assuming d-wave α-particle emission based on Rasmussen's approach [35].

From the three observed α-decay chains, the α-particle energy of ^{235}Bk was deduced to be 7632(17) keV. In these chains, ER-like events were observed within 30 s (see caption of Fig. 2). Although the half-life of ^{235}Bk cannot be reliably determined in the present experiment due to the measured time intervals being comparable to or longer than the average implantation time (~8 s), a lower limit on the order of several seconds is suggested. Assuming the α decay is g.s. to g.s. transition, the corresponding $Q_\alpha = 7764(17)$ and $Q_{\rm EC} = 4417(128)$ keV were deduced. A summary of the decay properties of ^{235}Bk and ^{231}Am are listed in Table 1. The extracted $Q_{\rm EC}$ values agree well with the FRDM2012 predictions [33] of 4.52 and 3.93 MeV for ^{235}Bk and ^{231}Am, respectively. The FRDM2012 model also predicts that the partial β-decay half-life $T^{\beta}_{1/2}$ for both nuclei are of the same order of magnitude as respective $T^{\alpha}_{1/2}$ values, which suggests their comparable α- and EC-decay branches in these two nuclei. This is consistent with the observed significant EC decay branch in ^{231}Am. We note that the daughter nucleus ^{235}Cm, from EC decay of ^{235}Bk, has small α-decay branch (1%) [37] which makes it difficult to be detected in the present experiment.

According to the FRDM calculations, the fission barriers B_f of ^{235}Cm and ^{231}Pu are 3.23 and 3.05 MeV [1], respectively. Taking into account the low $Q_{\rm EC} - B_f$ values (1.187 MeV for ^{235}Bk and 0.879 MeV for ^{231}Am) and the fission hindrance for the odd-A daughter nucleus [7], no ECDF branch is expected in these two isotopes, as confirmed by this experimental results.

As the branching ratio could not be determined for ^{235}Bk, we adopt a provisional assumption of 100% α-decay branching ratio for estimation purposes. Consequently, the *apparent* production cross sections were estimated as 1.4 pb at 182.4 MeV and 2.1 pb at 187.5 MeV, taking into account the 86(8)% α-particle detection efficiency, and 30% SHANS2 transmission efficiency (deduced from Monte Carlo simulations [38]). It should be noted that, however, depending on the actual α-decay branching ratio, the true production cross section could be much higher.

Fig. 4 presents a systematic comparison between the maximum experimental Q_α values of neutron-deficient Np-Cf isotopes and the theoretical g.s. to g.s. $Q^{\rm th}_\alpha$ from the Weizsäcker-Skyrme model together with the Radial Basis Function corrections (WS4 + RBF) [36]. The experimental Q_α values were derived from maximum α-particle energies from

NNDC database [20] and the present experimental results. As shown in Fig. 4, the WS4 + RBF model agrees well with the experimental data for most even-Z Pu, Cm, and Cf isotopes and odd-Z Np isotopes, and successfully reproduces the overall evolution trend of Q_α values. For odd-Z Bk and Am isotopes, however, the theoretical values are systematically larger than the experimental ones except for ^{234}Bk and ^{235}Am. Moreover, the predicted trend for Bk diverges significantly from the observed behavior. These discrepancies may arise from the complex level structure characteristic of odd-Z nuclei, in particular, feeding into excited states in the daughter nuclei, or may point to other underlying reasons, such as the inconsistencies of the model. Further experimental data in this region will be essential to clarify these systematic deviations.

4. Summary

In summary, the new isotopes, ^{235}Bk and its α-decay daughter ^{231}Am, were identified at the SHANS2 setup via the reaction ^{197}Au(^{40}Ar, 2n)^{235}Bk at the beam energies of 182.4 and 187.5 MeV, respectively. Three correlated α-decay chains were attributed to ^{235}Bk. The α-particle energies were determined to be 7632(17) keV for ^{235}Bk and 7109(18) keV for ^{231}Am. The half-life of ^{231}Am was measured as 75^{+137}_{-30} s. The α-decay branching ratio for ^{231}Am was evaluated to be 17^{+65}_{-15}%. The systematics of the α-decay Q-values were discussed, revealing significant discrepancies between the experimental values for odd-Z Bk and Am isotopes and the predictions of the WS4 + RBF model, which warrant further investigation.

Data availability

Data will be made available on request.

Declaration of competing interest

The authors declare that they have no known competing financial interests or personal relationships that could have appeared to influence the work reported in this paper.

Acknowledgments

The authors would like to thank the accelerator staff of CAFE2 for providing the stable ^{40}Ar beam. This work was supported in part by the National Key Research and Development Program of China (Contract Nos. 2023YFA1606500 and 2024YFE0110400), the Strategic Priority Research Program of Chinese Academy of Sciences (Grant No. XDB1550000), the Gansu Key Project of Science and Technology (Grant No. 23ZDGA014), the Guangdong Major Project of Basic and Applied Basic Research (Grant No. 2021B0301030006), the National Natural Science Foundation of China (Grants Nos. 12475126, W2412040, 12422507, 12535009, 12375118, 12435008, and W2412043), the CAS Project for Young Scientists in Basic Research (Grant No. YSBR-002), the Youth Innovation Promotion Association of the Chinese Academy of Sciences (Grants No. 2023439), and the Russian Science Foundation (Grant No. 25-42-00003). A.N.A. and A.A.V. were partially supported by Chinese Academy of Sciences President's International Fellowship Initiative Grants No. 2026PVA0208 and 2026PVA0049, respectively.

References

[1] P. Möller, A.J. Sierk, T. Ichikawa, A. Iwamoto, R. Bengtsson, H. Uhrenholt, S. Åberg, Heavy-element fission barriers, Phys. Rev. C 79 (2009) 064304. https://doi.org/10.1103/PhysRevC.79.064304

[2] P. Möller, A.J. Sierk, T. Ichikawa, A. Iwamoto, M. Mumpower, Fission barriers at the end of the chart of the nuclides, Phys. Rev. C 91 (2015) 024310. https://doi.org/10.1103/PhysRevC.91.024310

[3] M. Wang, W.J. Huang, F.G. Kondev, G. Audi, S. Naimi, The AME 2020 atomic mass evaluation (II). Tables, graphs and references*, Chin. Phys. C 45 (3) (2021) 030003. https://doi.org/10.1088/1674-1137/abddaf

[4] P. Möller, A.J. Sierk, T. Ichikawa, H. Sagawa, Nuclear ground-state masses and deformations: FRDM(2012), At. Data Nucl. Data Tables 109-110 (2016) 1–204. https://doi.org/10.1016/j.adt.2015.10.002

[5] G.L. Wilson, M. Takeyama, A.N. Andreyev, B. Andel, S. Antalic, W.N. Catford, L. Ghys, H. Haba, F.P. Heßberger, M. Huang, D. Kaji, Z. Kalaninova, K. Morimoto, K. Morita, M. Murakami, K. Nishio, R. Orlandi, A.G. Smith, K. Tanaka, Y. Wakabayashi, S. Yamaki, β-delayed fission of ^{230}Am, Phys. Rev. C 96 (2017) 044315. https://doi.org/10.1103/PhysRevC.96.044315

[6] J. Khuyagbaatar, β (EC) delayed fission in the heaviest nuclei, Eur. Phys. J. A 55 (8) (2019) 134. https://doi.org/10.1140/epja/i2019-12824-1

[7] A.N. Andreyev, M. Huyse, P. Van Duppen, Colloquium: Beta-delayed fission of atomic nuclei, Rev. Mod. Phys. 85 (2013) 1541–1559. https://doi.org/10.1103/RevModPhys.85.1541

[8] M. Sakama, K. Tsukada, M. Asai, S. Ichikawa, H. Haba, S. Goto, Y. Oura, I. Nishinaka, Y. Nagame, M. Shibata, et al., New isotope ^{233} Am, Eur. Phys. J. A 9 (3) (2000) 303–305. https://doi.org/10.1007/s100500070013

[9] M. Sakama, M. Asai, K. Tsukada, S. Ichikawa, I. Nishinaka, Y. Nagame, H. Haba, S. Goto, M. Shibata, K. Kawade, Y. Kojima, Y. Oura, M. Ebihara, H. Nakahara, α-decays of neutron-deficient americium isotopes, Phys. Rev. C 69 (2004) 014308. https://doi.org/10.1103/PhysRevC.69.014308

[10] D. Kaji, K. Morimoto, H. Haba, E. Ideguchi, H. Koura, K. Morita, Decay Properties of New Isotopes ^{234} Bk and ^{230} Am, and Even–Even Nuclides ^{234} Cm and ^{230} Pu, J. Phys. Soc. Jpn. 85 (1) (2016) 015002. https://doi.org/10.7566/JPSJ.85.015002

[11] V.I. Kuznetsov, N.K. Skobelev, G.N. Flerov, Spontaneously fissile neutron-deficient neptunium isotope with 60-sec half-life, Sov. J. Nucl. Phys. 4 (2) (1967) 202.

[12] D. Habs, H. Klewe-Nebenius, V. Metag, B. Neumann, H.J. Specht, Determination of the fission barrier of ^{232} Pu from β-delayed fission and the problem of the first barrier, Z. Phys. A 285 (1) (1978) 53–57. https://doi.org/10.1007/BF01410224

[13] H.L. Hall, K.E. Gregorich, R.A. Henderson, C.M. Gannett, R.B. Chadwick, J.D. Leyba, K.R. Czerwinski, B. Kadkhodayan, S.A. Kreek, N.J. Hannink, D.M. Lee, M.J. Nurmia, D.C. Hoffman, C.E.A. Palmer, P.A. Baisden, Electron-capture-delayed fission properties of ^{232}Am, Phys. Rev. C 42 (1990a) 1480–1488. https://doi.org/10.1103/PhysRevC.42.1480

[14] H.L. Hall, K.E. Gregorich, R.A. Henderson, C.M. Gannett, R.B. Chadwick, J.D. Leyba, K.R. Czerwinski, B. Kadkhodayan, S.A. Kreek, D.M. Lee, M.J. Nurmia, D.C. Hoffman, C.E.A. Palmer, P.A. Baisden, Electron-capture-delayed fission properties of ^{234}Am, Phys. Rev. C 41 (1990b) 618–630. https://doi.org/10.1103/PhysRevC.41.618

[15] H.M. Devaraja, S. Heinz, O. Beliuskina, V. Comas, S. Hofmann, C. Hornung, G. Münzenberg, K. Nishio, D. Ackermann, Y.K. Gambhir, M. Gupta, R.A. Henderson, F.P. He?berger, J. Khuyagbaatar, B. Kindler, B. Lommel, K.J. Moody, J. Maurer, R. Mann, A.G. Popeko, D.A. Shaughnessy, M.A. Stoyer, A.V. Yeremin, Observation of new neutron-deficient isotopes with Z ≥ 92 in multinucleon transfer reactions, Phys. Lett. B 748 (2015) 199–203. https://doi.org/10.1016/j.physletb.2015.07.006

[16] J. Konki, J. Khuyagbaatar, J. Uusitalo, P.T. Greenlees, K. Auranen, H. Badran, M. Block, R. Briselet, D.M. Cox, M. Dasgupta, A. Di Nitto, C.E. Düllmann, T. Grahn, K. Hauschild, A. Herzán, R.-D. Herzberg, F.P. Heßberger, D.J. Hinde, R. Julin, S. Juutinen, E. Jäger, B. Kindler, J. Krier, M. Leino, B. Lommel, A. Lopez-Martens, D.H. Luong, M. Mallaburn, K. Nishio, J. Pakarinen, P. Papadakis, J. Partanen, P. Peura, P. Rahkila, K. Rezynkina, P. Ruotsalainen, M. Sandzelius, J. Sarén, C. Scholey, J. Sorri, S. Stolze, B. Sulignano, C. Theisen, A. Ward, A. Yakushev, V. Yakusheva, Towards saturation of the electron-capture delayed fission probability: The new isotopes ^{240} Es and ^{236}Bk, Phys. Lett. B 764 (2017) 265–270. https://doi.org/10.1016/j.physletb.2016.11.038

[17] S.A. Kreek, H.L. Hall, K.E. Gregorich, R.A. Henderson, J.D. Leyba, K.R. Czerwinski, B. Kadkhodayan, M.P. Neu, C.D. Kacher, T.M. Hamilton, M.R. Lane, E.R. Sylwester, A. Türler, D.M. Lee, M.J. Nurmia, D.C. Hoffman, Electron-capture delayed fission properties of the new isotope ^{238}Bk, Phys. Rev. C 49 (1994) 1859–1866. https://doi.org/10.1103/PhysRevC.49.1859

[18] L.N. Sheng, Q. Hu, H. Jia, Z.Y. Zhang, Z. Chai, B. Zhao, Y. Zhang, Z.G. Gan, Y. He, J.C. Yang, Ion-optical design and multiparticle tracking in 3D magnetic field of the gas-filled recoil separator SHANS2 at CAFE2, Nucl. Instrum. Methods Phys. Res., Sect. A 1004 (2021) 165348. https://doi.org/10.1016/j.nima.2021.165348

[19] S.Y. Xu, Z.Y. Zhang, Z.G. Gan, M.H. Huang, L. Ma, J.G. Wang, M.M. Zhang, H.B. Yang, C.L. Yang, Z. Zhao, X.Y. Huang, L.X. Chen, X.J. Wen, H. Zhou, H. Jia, L.N. Sheng, J.Q. Wu, X.L. Peng, Q. Hu, J. Yang, Q.G. Yao, Y.S. Qin, H.H. Yan, Z. Chai, J.C. Zhang, Y. Zhang, Z. Du, H.M. Xie, B. Zhao, G.Z. Sun, F.F. Wang, C.Z. Yuan, X.L. Wu, R.F. Chen, H.B. Zhang, Z.W. Lu, H.R. Yang, X.X. Xu, Y.X. Chen, A.H. Feng, P. Sun, J.K. Xu, Y. He, L.T. Sun, X.H. Zhou, H.S. Xu, V.K. Utyonkov, A.A. Voinov, Y.S. Tsyganov, A.N. Polyakov, D.I. Solovyev, A gas-filled recoil separator, SHANS2, at the China Accelerator Facility for Superheavy Elements, Nucl. Instrum. Methods Phys. Res., Sect. A 1050 (2023) 168113. https://doi.org/10.1016/j.nima.2023.168113

[20] N.N.D. Center, Information extracted from the NuDat database. https://www.nndc.bnl.gov/nudat/.

[21] V.T. Jordanov, G.F. Knoll, Digital synthesis of pulse shapes in real time for high resolution radiation spectroscopy, Nucl. Instrum. Methods Phys. Res., Sect. A 345 (2) (1994) 337–345. https://doi.org/10.1016/0168-9002(94)91011-1

[22] H.B. Yang, Z.G. Gan, Z.Y. Zhang, M.M. Zhang, M.H. Huang, L. Ma, C.L. Yang, A digital pulse fitting method for the α decay studies of short-lived nuclei, Eur. Phys. J. A 55 (1) (2019) 8. https://doi.org/10.1140/epja/i2019-12684-7

[23] A.K. Mistry, J. Khuyagbaatar, F.P. Heßberger, D. Ackermann, B. Andel, S. Antalic, M. Block, P. Chhetri, F. Dechery, C. Droese, C.E. Düllmann, F. Giacoppo, J. Hoffmann, O. Kaleja, N. Kurz, M. Laatiaoui, L. Lens, J. Maurer, P. Mosat, J. Piot, S. Raeder, M. Vostinar, A. Yakushev, Z. Zhang, The 48Ca + 181Ta reaction: Cross section studies and investigation of neutron-deficient 86 ≤ Z ≤ 93 isotopes, Nucl. Phys. A 987 (2019) 337–349. https://doi.org/10.1016/j.nuclphysa.2019.05.003

[24] A.A. Kuznetsova, A.I. Svirikhin, A.V. Isaev, M.A. Bychkov, V.D. Danilkin, H.M. Devaraja, N.I. Zamyatin, I.N. Izosimov, Z. Liu, O.N. Malyshev, et al., Properties of Radioactive Decay of the New Nucleus ^{227}Pu, Phys. Part. Nuclei Lett. 22 (2) (2025) 406–412. https://doi.org/10.1134/S1547477124702510

[25] W. Reisdorf, Analysis of fissionability data at high excitation energies: I. The level density problem, Z. Phys. A 300 (2) (1981) 227–238. https://doi.org/10.1007/BF01412298

[26] V. Ninov, F.P. Hessberger, P. Armbruster, S. Hofmann, G. Münzenberg, M. Leino, Y. Fujita, D. Ackermann, W. Morawek, A. Lüttgen, Identification of neutron-deficient isotopes ^{226,227} Np, Z. Phys. A 336 (4) (1990) 473–474. https://doi.org/10.1007/BF01294121

[27] F. Hoellinger, B.J.P. Gall, N. Schulz, N. Amzal, P.A. Butler, P.T. Greenlees, D. Hawcroft, J.F.C. Cocks, K. Helariutta, P.M. Jones, R. Julin, S. Juutinen, H. Kankaanpää, H. Kettunen, P. Kuusiniemi, M. Leino, M. Muikku, D. Savelius, Electromagnetic transitions and α decay of the ^{223}Pa nucleus, Phys. Rev. C 60 (1999) 057301. https://doi.org/10.1103/PhysRevC.60.057301

[28] J. Borggreen, K. Valli, E.K. Hyde, Production and Decay Properties of Protactinium Isotopes of Mass 222 to 225 Formed in Heavy-ion Reactions, Phys. Rev. C 2 (1970) 1841–1862. https://doi.org/10.1103/PhysRevC.2.1841

[29] C.A. Laue, K.E. Gregorich, R. Sudowe, M.B. Hendricks, J.L. Adams, M.R. Lane, D.M. Lee, C.A. McGrath, D.A. Shaughnessy, D.A. Strellis, E.R. Sylwester, P.A. Wilk, D.C. Hoffman, New plutonium isotope: ^{231}Pu, Phys. Rev. C 59 (1999) 3086–3092. https://doi.org/10.1103/PhysRevC.59.3086

[30] J. Khuyagbaatar, F.P. Heßberger, S. Hofmann, D. Ackermann, H.G. Burkhard, S. Heinz, B. Kindler, I. Kojouharov, B. Lommel, R. Mann, J. Maurer, K. Nishio, α decay of ^{243}Fm$_{143}$ and ^{245}Fm$_{145}$, and of their daughter nuclei, Phys. Rev. C 102 (2020) 044312. https://doi.org/10.1103/PhysRevC.102.044312

[31] K.-H. Schmidt, C.-C. Sahm, K. Pielenz, H.G. Clerc, Some remarks on the error analysis in the case of poor statistics, Z. Phys. A 316 (1) (1984) 19–26. https://doi.org/10.1007/BF01415656

[32] M. Asai, M. Sakama, K. Tsukada, S. Ichikawa, H. Haba, I. Nishinaka, Y. Nagame, S. Goto, Y. Kojima, Y. Oura, et al., EC and α decays of ^{235} Am, Eur. Phys. J. A 22 (3) (2004) 411–416. https://doi.org/10.1140/epja/i2004-10044-6

[33] P. Möller, M.R. Mumpower, T. Kawano, W.D. Myers, Nuclear properties for astrophysical and radioactive-ion-beam applications (II), At. Data Nucl. Data Table 125 (2019) 1–192. https://doi.org/10.1016/j.adt.2018.03.003

[34] Y. Ren, Z. Ren, New Geiger-Nuttall law for α decay of heavy nuclei, Phys. Rev. C 85 (2012) 044608. https://doi.org/10.1103/PhysRevC.85.044608

[35] J.O. Rasmussen, Alpha-decay Barrier Penetrabilities with an Exponential Nuclear Potential: Even-even Nuclei, Phys. Rev. 113 (1959) 1593–1598. https://doi.org/10.1103/PhysRev.113.1593

[36] N. Wang, M. Liu, X. Wu, J. Meng, Surface diffuseness correction in global mass formula, Phys. Lett. B 734 (2014) 215–219. https://doi.org/10.1016/j.physletb.2014.05.049

[37] J. Khuyagbaatar, F.P. Heßberger, S. Hofmann, D. Ackermann, H.G. Burkhard, S. Heinz, B. Kindler, I. Kojouharov, B. Lommel, R. Mann, J. Maurer, K. Nishio, α decay of ^{243}Fm$_{143}$ and ^{245}Fm$_{145}$, and of their daughter nuclei, Phys. Rev. C 102 (2020) 044312. https://doi.org/10.1103/PhysRevC.102.044312

[38] M.M. Zhang, D.I. Solovyev, S. Kuzovlev, S.Y. Xu, Z.Y. Zhang, Z.G. Gan, Monte Carlo simulation of recoil trajectories in the gas-filled recoil separator SHANS2 using Geant4 toolkit, Nucl. Instrum. Methods Phys. Res., Sect. A 1086 (2026) 171376. https://doi.org/10.1016/j.nima.2026.171376